

RNAi Silenced *Dd-grp94* (*Dictyostelium discoideum* Glucose-Regulated Protein 94 kDa) Cell Lines in *Dictyostelium* Exhibit Marked Reduction in Growth Rate and Delay in Development

SANDHYA N. BAVISKAR* AND MALCOLM S. SHIELDS†

*Department of Biological Sciences, University of Arkansas-Fort Smith, Fort Smith, AR, USA

†Department of Biological Sciences, Idaho State University, Pocatello, ID, USA

Glucose-regulated 94 kDa protein (Grp94) is a resident of the endoplasmic reticulum (ER) of multicellular eukaryotes. It is a constitutively expressed protein that is overexpressed in certain abnormal conditions of the cell such as depletion of glucose and calcium, and low oxygen and pH. The protein is also implicated in diseased conditions like cancer and Alzheimer's disease. In this study, the consequences of downregulation of Grp94 were investigated at both unicellular and multicellular stages of *Dictyostelium discoideum*. Previous studies have shown the expression of *Dd-Grp94* (*Dictyostelium discoideum* glucose-regulated 94 kDa protein) in wild-type cells varies during development, and overexpression of *Dd-Grp94* leads to abnormal cell shape and inhibition of development (i.e., formation of fruiting bodies). Grp94 is a known calcium binding protein and an efficient calcium buffer. Therefore, in the present study we hypothesized that downregulation of *Dd-Grp94* protein would affect *Dictyostelium* cell structure, growth, and development. We found that *Dd-grp94* RNAi recombinants exhibited reduced growth rate, cell size, and a subtle change in cell motility compared to the parental cells. The recombinants also exhibited a delay in development and small fruiting bodies. These results establish that *Dd-grp94* plays a crucial role in determining normal cell structure, growth and differentiation.

Key words: *Dictyostelium discoideum* glucose-regulated 94 kDa protein (*Dd-Grp94*); RNA interference; Glucose-regulated 94 kDa protein (Grp94); Endoplasmic reticulum

INTRODUCTION

Glucose-regulated protein 94 kDa (Grp94) is the most abundant protein of endoplasmic reticulum (ER) found only in multicellular organisms with its no orthologs in unicellular organisms (2,20). It is a low-affinity, high-capacity calcium binding protein and an efficacious calcium buffer (2,4). Grp94 is constitutively expressed in all tissues but overexpressed in abnormal metabolic conditions such as depletion of glucose and calcium, low oxygen, low pH, and in

the presence of some mutated proteins and during viral infections (2,3,15,16). It is a homodimer consisting of 781 amino acid residues and each protomer of the homodimer has N-terminal regulatory domain that has an ATP-binding and a peptide-binding site, a middle domain comprised of negatively charged residues, and a C-terminal dimerization domain (40). It is considered as a molecular chaperone owing to its sequence homology and structural similarity with cytosolic Hsp90 (heat shock protein) family of proteins (25). There is a conclusive evidence that, like

Address correspondence to Sandhya N. Baviskar, Department of Biological Sciences, University of Arkansas-Fort Smith, 5210 Grand Avenue, Fort Smith, AR 72913, USA. Tel: 479-788-7789; Fax: 479-788-7612; E-mail: sbaviska@uafortsmith.edu

Hsp90, Grp94 is an ATP hydrolyzing enzyme but the rate of hydrolysis is 5–25-fold slower than Hsp90 (10). Grp94 is suggested to have chaperone function as it is known to be associated with the late folding stages of proteins (Ig light chain) *in vitro*, although its chaperone activity has not been demonstrated *in vivo* (10,25). It also binds and presents immunological peptides such as IgG, integrins, and Toll-like receptors (25,31,49).

Because Grp94 is implicated in several diseases such as goiter, Alzheimer's disease, lung cancer, breast cancer, and immune disorders (20,28,34,35, 44,47), many researchers have attempted to elucidate the functions of Grp94 in different organisms and cell lines using a variety of techniques. Elimination of *Grp94* gene (by knockout) in mouse embryos is lethal (41). In another study (46), murine *Grp94* gene disruption caused embryonic lethality because mesoderm, primitive streak, and preamniotic cavity failed to develop. This study further showed that *Grp94* affects embryonic development by regulating the secretion of insulin-like growth factor-II (IGF-II). It has been found that Grp94 is involved in complex glycosylation of prion (PrP) protein in neuroblastoma (N2a) cells. In *Arabidopsis*, knockout of Grp94 affects its development (14).

In this study, we elucidate the functions of *Grp94* gene in eukaryotic model organism *Dictyostelium discoideum*. During its life cycle, *Dictyostelium* exist as unicellular and multicellular life forms (17). In nature, they are found in forest soils where they feed on bacteria and yeast and reproduce asexually by binary fission (12). During vegetative phase of its life cycle, *Dictyostelium* cells are solitary, free-living amoebae feeding on bacteria. Depletion of food causes *Dictyostelium* cells to enter the developmental phase, during which starving cells aggregate to form multicellular fruiting bodies. Each fruiting body is approximately 1–2 mm long and has a multicellular stalk and a spore. In the presence of nutrients and suitable environmental conditions, each spore cell develops into a unicellular amoeba (12,18). *Dictyostelium* regulate their cell density in relation to food density by secreting a glycoprotein called prestarvation factor (PSF) (33). Normally, vegetatively grown amoebae secrete PSF but their response to PSF is inhibited by bacteria (food). When the food is scarce in relation to cell density, the concentration of PSF increases, which in turn induces the genes that cause *Dictyostelium* to enter the developmental (multicellular) phase of the life cycle (33). Aggregation of starving amoebae occurs by chemotaxis to cAMP (3'-5' cyclic adenosine mononucleotide phosphate; cAMP) signals. A few amoebae start producing cAMP and form the aggregation

center. The cAMP signal is detected, amplified, and relayed by the G-protein-coupled receptors present on the cell surface of the neighboring starving cells. Approximately 10^5 cells move towards increasing cAMP concentrations and form a hemispherical cluster called a "mound," which eventually differentiates into a multicellular fruiting body (18,21).

Grp94 is an efficacious calcium buffer (45) and its activity is regulated by calcium (1,4), which is a well-established regulator of actin cytoskeleton structure and dynamics (5,7,13). The diverse processes that the actin cytoskeleton affects in a cell include morphogenesis, cell motility, cell division, phagocytosis, and exocytosis (6,13,19,29,42). Various studies have shown increased level of intracellular calcium (Ca^{2+}_i) and related decreased level of sequestered Ca^{2+} in high-capacity calcium stores (endoplasmic reticulum) in differentiating *Dictyostelium* cells (5,51). It has been found that during development, differentiation-inducing factor (DIF) causes increase in Ca^{2+}_i , which leads to the activation of pre-stalk-specific *ecmB* gene expression by some unknown mechanism (5). In a previous study, Morita et al. (27) showed that the *Dd-grp94* overexpressed cells had abnormal cell shape and their development into spores and stalk was inhibited. Because regulation of Grp94 by calcium and its involvement in *Dictyostelium* development has been shown by previous studies (4,5,13,26), we hypothesized that complete or partial elimination of *Dd-Grp94* would affect calcium binding cytoskeletal proteins, which would in turn affect *Dictyostelium* cell structure, growth, and development.

In this study, RNAi was the method of choice to explore *Dd-grp94* functions as the other methods (antisense-mediated gene silencing and gene disruption by homologous recombination) had failed [(27), unpublished results by Baviskar and Shields]. RNAi technique is accurate, target specific, and well established in *Dictyostelium* research (23). A hairpin RNA construct targeted against *Dd-grp94* gene was constructed using gene expression system comprising of two plasmids vectors [transactivator plasmid (pMB35) and an extrachromosomal response plasmid (pMB38)]. The transcriptional activator protein (tTA), produced by the integrating plasmid (pMB35), binds specifically to the tetracycline response element (TRE) on the extrachromosomal plasmid (pMB38) and activates the promoter leading to the transcription of the gene of interest.

Our study shows that the *Dd-grp94* RNAi recombinants exhibited reduced growth rate, cell size, and a subtle change in cell motility compared to the parental cells. The recombinants also exhibited delayed development and produced small fruiting bodies.

MATERIALS AND METHODS

Construction of the Dd-grp94 RNAi Vector (pMSB08)

The steps to produce the *Dd-grp94* RNAi vector are shown in Figure 1. Two fragments differing in length by 113 bp were amplified from the unique region of the *Dd-grp94* gene using the primers with suitable restriction sites (see Table 1) and ligated to each other in reverse orientation. The ligated fragment (1249 bp) was cloned into a *Bgl*III/*Sph*I-digested pMB38 vector. The resulting plasmid pMSB08 had the construct with inverted repeats of the same *Dd-grp94* sequences separated by 113 bp of unshared material. The construct folds into a 568-bp double-

stranded stem-loop structure and the 113-bp unpaired region forms the hair-pin loop. The vector thus constructed (pMSB08) was electroporated into MB35 cells (AX2 wild-type cells transformed with transactivator plasmid pMB35) (8) to obtain the *Dd-grp94* RNAi recombinants.

Dictyostelium discoideum Cell Culture and Transformation

MB35 cell culture was maintained in HL-5 medium (10 g dextrose, 10 g proteose peptone, 5 g yeast extract, 0.97 g Na₂HPO₄, 0.48 g KH₂PO₄, and 0.03 g streptomycin, volume to 1 L and autoclaved) supplemented with G418-sulphate (GIBCO Invitrogen Inc.,

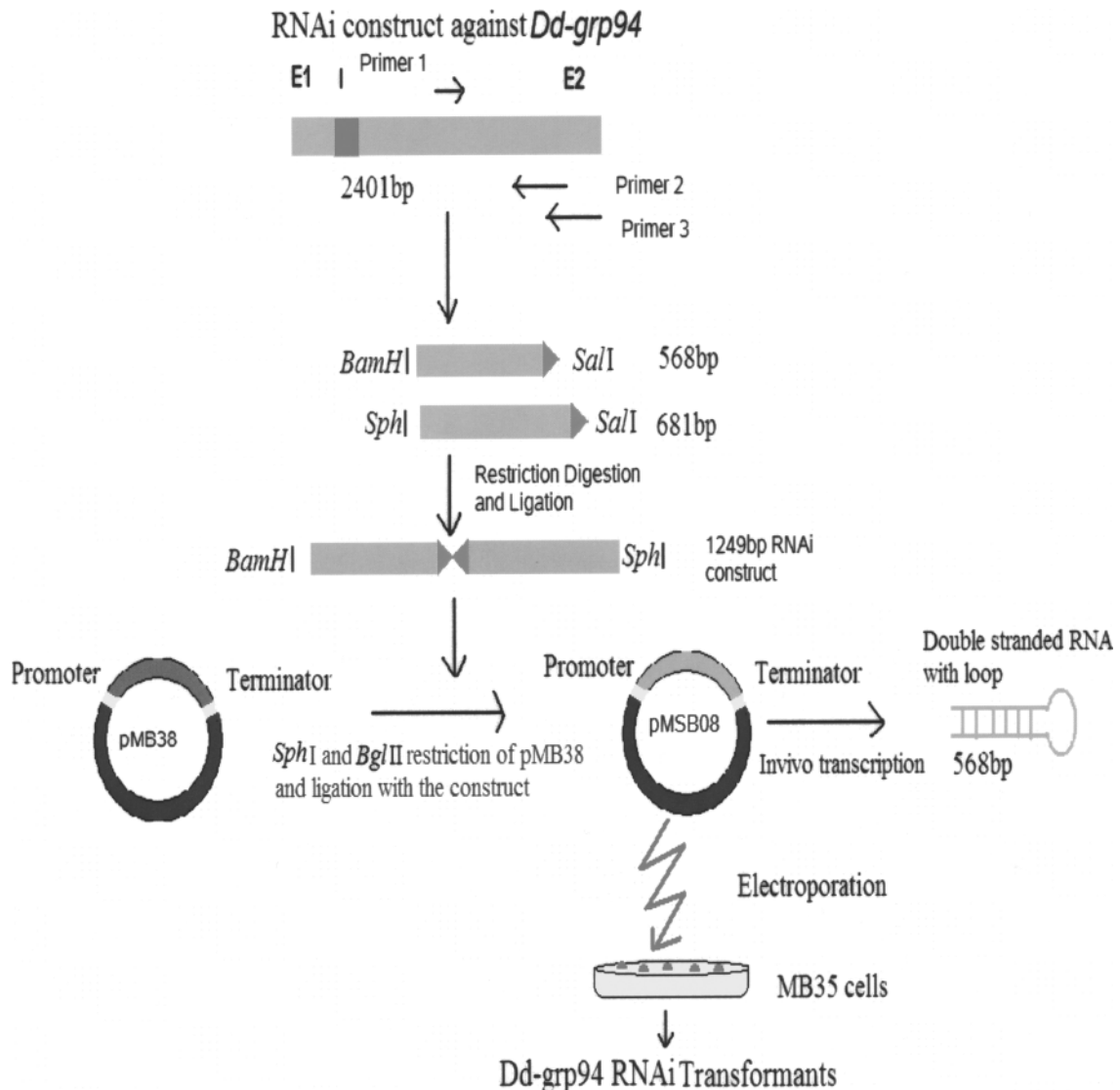


Figure 1. Schematic diagram of the construction of the *Dd-grp94* RNAi vector.

TABLE 1
POLYMERASE CHAIN REACTION PRIMERS

Primer Name	PCR Primers Nucleotide Sequence 5'–3'	Target	Sequence Length
Sfgrp94sphI	GCGGCATGCGGAATTGGTTCCAAATTGGTT	<i>Dd-grp94</i> base (1203–1223)	568 base pairs
Snrgrp94SalI	GCGGTCGACTTACGTTGATCCTCTTCCTC	<i>Dd-grp94</i> base (1747–1767)	
fgrp94BamHI	GCGGGATCCGGAATTGGTTCCAAATTGGTT	<i>Dd-grp94</i> base (1203–1223)	681 base pairs
rgrp94SalI	GCGGTCGACACTAAAATACTTGGTGAGTCAGC	<i>Dd-grp94</i> base (1858–1880)	
GAPDHFor	GGTTGTCCCAATTGGTATTAATGG	<i>Dd-gpdA</i> base (3–26)	247 base pairs
GAPDHRev	CCGTGGGTTGAATCATATTTGAAC	<i>Dd-gpdA</i> base (224–247)	
grpF-rtPCR	ATACACAGAAGCTGAAGCAAA	<i>Dd-grp94</i> base (108–128)	445 base pairs
grpR-rtPCR	ATTCTTTAGTTCCTGATTGGG	<i>Dd-grp94</i> base (532–552)	

Grand Island, NY) at a final concentration of 5 µg/ml and maintained at 22°C. Transformation by electroporation was performed by modifications to the protocol of Schlatterer et al. (38). Approximately 5 × 10⁶ cells were pelleted by centrifugation (Sorvall TC, Dupont Inc., USA) at 2000 × *g* for 2 min and suspended in 1 ml ice-cold H-50 buffer (20 mM HEPES, 50 mM KCl, 10 mM NaCl, 1 mM MgSO₄, 5 mM NaHCO₃, 1 mM NaH₂PO₄ autoclaved and stored at –20°C, pH 7). The cell pellet was suspended in 70 µl of ice-cold H-50 buffer after washing twice with 1 ml of H-50 buffer. Approximately 10 µg (40 µl) of pMSB08 (*Dd-grp94* RNAi vector) was added to a 70 µl cell suspension and transferred to a 0.1 cm cold electroporation cuvette and electroporated using Bio-Rad Gene Pulser II (0.5 kV/cm, 10 µF, 50 Ohms) (Bio-Rad Inc., Hercules, CA) for 6 s. One milliliter of HL-5 medium was added to the cells in the cuvette, allowed to recover at room temperature for 15 min, and then transferred to 100-mm petri dish containing 10 ml of HL-5 medium. Twenty-four hours after electroporation, G418-sulphate (GIBCO Invitrogen Inc.) and Blasticidin S (Fisher Scientific, Fair Lawn, NJ) were added to the cells (after changing the medium) each to a final concentration of 5 µg/ml. The transformants obtained after a week were clonally isolated by twofold serial dilution in 96-well microtiter plate (Corning Inc., NY, USA). Three clonally isolated *Dd-Grp94* RNAi recombinant cell lines, namely C4, C7, and C14, were analyzed for growth rate, size, and development and compared with MB35 (parental) cells.

Cell Proliferation Assay

For measuring cell proliferation, MB35 cells and the recombinant cell lines were shaken in a 250-ml conical flask containing 50 ml of HL-5 medium supplemented with antibiotics (G418 and Blasticidin S each at a final concentration of 5 µg/ml each) at 40 rpm at 22°C. The initial cell density was 1 × 10⁵

cells/ml and thereafter it was measured at an interval of 24 h for 5 days (104 hours) using a hemacytometer. From an average of three experiments for each cell line, the mean generation time during exponential growth for each cell line was determined.

Cell Size Assay

Starvation induces individual *Dictyostelium* cells to move fast towards each other but when grown in axenic nutrient medium in a petri dish, they move very slowly and stick to the bottom of the plate. To estimate cell size, the parental cells (MB35 cells) and the recombinant cell lines were grown in 100-mm petri dish in axenic nutrient medium for about 1 day. The next day, the medium was aspirated to remove dead and floating cells and immediately (before the plate dried) pictures of the cells were taken from different regions of the plate using a CCD camera (Sony Inc., USA) attached to the inverted microscope (Olympus CK 2, Olympus America Inc., Melville, NY) at 20× magnification. A sample size of 1,000 cells was evaluated for each cell line using ImageJ software (32). Individual cell areas were calculated in µm² and exported into Excel file format for analysis.

Cell Speed Assay

The rate of amoeboid movement of MB35 cells and the three clonal cell lines was estimated by analyzing the time-lapse movies made by capturing the bright field images of the cells for specific time period during development. For each cell line, 2 × 10⁷ cells were harvested, pelleted by centrifugation (Sorvall TC, DuPont Inc.) at 2000 rpm for 2 min, and washed with development buffer (5 mM Na₂HPO₄, 5 mM KH₂PO₄, 1 mM CaCl₂, 2 mM MgCl₂, pH 6.5, stored at 4°C) twice and suspended in 20 ml of development buffer in a 250 ml conical flask and shaken at 40 rpm at 22°C for 5.5 h. After 5.5 and 6.5 h of starvation, a small aliquot of cells was allowed to ad-

here to 100-mm petri dish for 5 min and then bright field images of the moving cells were taken for 30 min at 20× magnification using the CCD camera (Sony Inc.) attached to the inverted microscope (Olympus CK 2, Olympus America Inc.) and also to a computer with video capture card. The videos, made for each cell line at two different times (5.5 and 6.5 h starvation), were decompiled using VirtualDub 1.8.6 software and 40 picture frames were picked manually at the intervals of 45 s. Ten randomly selected cells (for each time point and for each cell line) were digitized (x and y coordinates obtained for each cell from first frame to the last) using Didge software and the distance covered was determined using the distance formula: $[(x_2 - x_1)^2 + (y_2 - y_1)^2]^{1/2}$.

Development Assay

The clonally isolated populations of treated and control cells were induced to undergo development on solid substratum to compare their developmental stages. For each cell line, 2×10^8 cells were washed twice with ice-cold development buffer (5 mM Na_2HPO_4 , 5 mM KH_2PO_4 , 1 mM CaCl_2 , 2 mM MgCl_2 , pH 6.5, stored at 4°C) and spread on sterile KK2 starvation plates (2.2 g KH_2PO_4 , 0.7 g K_2HPO_4 , 15 g Agar/L) to undergo development. Pictures of MB35 and treated cell lines were taken at different times during development.

Real-Time PCR Analysis

Total RNA was extracted from approximately 2×10^6 cells from each of the three clonal populations and MB35 cells using Aurum™ Total RNA Mini Kit (Bio-Rad Laboratories Inc., Hercules, CA) following the manufacturer's instructions. Reverse transcription reaction was performed in 20 μl reaction volume on 1–2 μg of total RNA using Superscript III First Strand Synthesis for RT PCR (Invitrogen) following the manufacturer's instructions. Quantitative PCR (qPCR) was carried out in triplicate for each cell line in a 50- μl final reaction volume containing 1 μl each (300 nM) of forward primer: grpF-rtPCR and reverse primer: grpR-rtPCR (Table 1) and 25 μl of Quantitect 2X SYBR Green PCR master mix (Qiagen Inc., CA, USA) using Chromo4™ Real-Time PCR System (MJ Research, Boston, MA). The *Dd-grp94* primers flanked the intron containing 98 base pairs. For each cell line, *Dd-grp94* mRNA was quantified relative to *Dictyostelium* glyceraldehyde 3-phosphate dehydrogenase (*Dd-gpdA*) using the forward and reverse primers GAPDHFor and GAPDHRev, respectively (Table 1). The *Dd-gpdA* primers flanked the 91-base pair intron region. *Dd-gpdA* was used as an internal

control gene to normalize for *Dd-grp94* mRNA expression. The analyses of qPCR data were performed by Opticon Monitor software (MJ Research, Boston, MA).

RESULTS

Reduction in *Dd-grp94* mRNA Level

In order to ascertain the silencing of *Dd-grp94* gene in the recombinant cell lines, expression level of *Dd-grp94* mRNA was measured and compared with parental cells using real-time quantitative PCR. The standard curve method was used to calculate the relative expression of *Dd-grp94* in MB35 cells (parental) and *Dd-grp94* RNAi recombinant cell lines. Analyses of the data show 10-fold reduction in the mean expression level of *Dd-grp94* mRNA measurements triplicate recombinant cell lines (C4, C7, and C14) compared to the mean value from triplicate control parental cell lines (MB35 cells) (Fig. 2).

Cell Proliferation Assay

From an average of three experiments, the mean generation time during exponential growth was measured as number of hours per doubling. The doubling time for MB35 (parental cell line) was found to be 11.5 h and for cell lines C4, C7, and C14 the doubling time was 14.8, 17.3, and 17.3 h, respectively (Fig. 3). To determine if the difference in growth rate between the parental cell line and each of the recom-

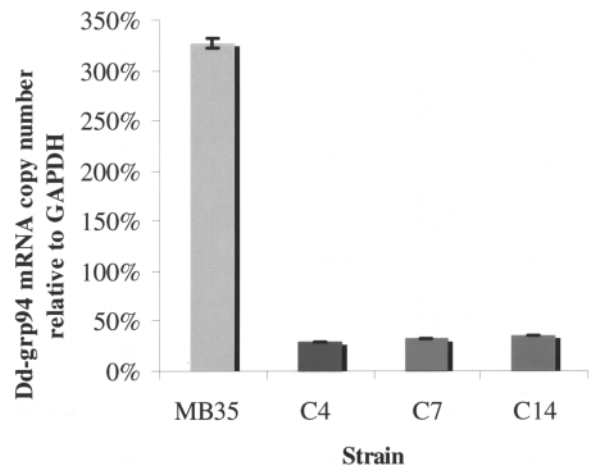


Figure 2. *Dd-grp94* expression by reverse transcriptase-quantitative PCR. Triplicate cultures of the wt MB35 and three RNAi recombinant cell lines (C4, C7, and C14) were analyzed for *Dd-grp94* mRNA copies relative to the housekeeping control gene *Dictyostelium* GAPDH (*Dd-gpdA*). SD: MB35 = $\pm 5.09\%$, C4 = $\pm 0.42\%$, C7 = $\pm 0.38\%$, C14 = $\pm 0.64\%$.

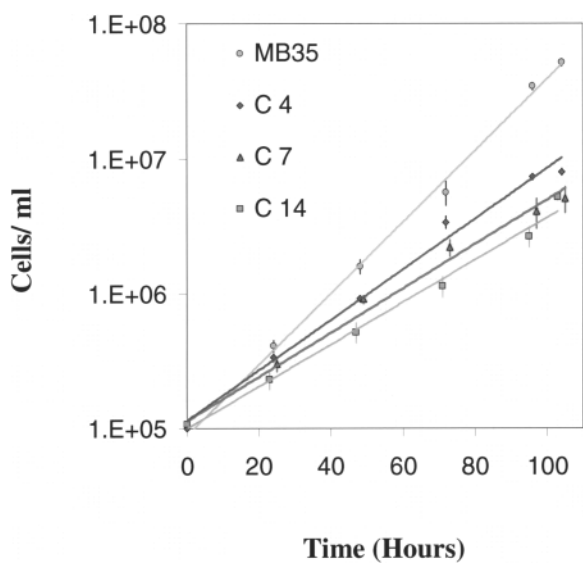


Figure 3. Growth rate of recombinant cell lines (C4, C7, and C14) is compared to MB35 cell line (parental) during exponential growth phase. The doubling time for MB35 was 11.5 h and for C4, C7, and C14 the doubling time was 14.8, 17.3, and 17.3 h, respectively. All data are presented as the mean \pm SD of three independent measurements.

binant cell lines was statistically significant, Student's *t* test was performed. The statistical tests (Table 2) suggested that the differences in growth rates of the parental cell line (MB35) and each of the recombinant cell lines were highly significant. It was concluded that downregulation of Dd-Grp94 protein suppresses cell proliferation rate.

Cell Size Assay

As these cell lines were a population of asynchronously dividing cells, their cell areas varied from 100 to 1500 μm^2 . Because of the wide range of variation in cell size in the recombinant and parental cell lines, the cells were grouped by size range and the number of cells in each size range was compared across the

cell lines (Figs. 4 and 5). The area of majority of the parental cells was within the range of 400–600 μm^2 (mean cell area = $542.38 \pm 12.43 \mu\text{m}^2$, STDEVP, $\sigma = 200.60 \mu\text{m}^2$), while most of the cells of C4 cell line fall within the range of 200–400 μm^2 (mean cell area = $318.76 \pm 5.80 \mu\text{m}^2$, STDEVP, $\sigma = 93.65 \mu\text{m}^2$). Likewise, the majority of the cells of cell lines C7 (mean cell area = $292.86 \pm 6.6 \mu\text{m}^2$, STDEVP, $\sigma = 107.51 \mu\text{m}^2$) and C14 (mean cell area = $241.64 \pm 5.43 \mu\text{m}^2$, STDEVP, $\sigma = 87.69 \mu\text{m}^2$) were within the range of 200–300 μm^2 . The confidence interval for the difference of two means was calculated to compare the cell size averages of the parental cell line (MB35) with each of the recombinant cell lines C4, C7, and C14 (at 95% confidence level). The confidence interval values for the difference of two means for C4, C7, and C14, when individually compared with MB35, were found to be 223.62 ± 13.72 , 249.52 ± 14.106 , and $300.74 \pm 13.56 \mu\text{m}^2$, respectively. The data clearly show that the cell size of *Dd-grp94* RNAi recombinants is reduced in comparison to parental cells (MB35).

Cell Speed Assay

Cell speed of MB35 (parental cells) and *Dd-grp94* recombinant cell lines at 5.5 and 6.5 h of starvation was estimated as described in Materials and Methods. There was no significant difference in the average cell speed of MB35 cells (Figs. 6 and 7) and the recombinant cell lines (C4, C7, C14) at 5.5 h of starvation ($n = 10$, $p = 0.640$) but a subtle difference was noted at 6.5 h of starvation. A single factor ANOVA was performed on all the results. The average cell speed at 5.5 h of starvation of MB35 cells was $4.8 \pm 0.36 \mu\text{m}/\text{min}$ (STDEV, $\sigma = 1.16 \mu\text{m}/\text{min}$) and that of recombinant cell lines C4 and C7 was $4.3 \pm 0.42 \mu\text{m}/\text{min}$ (STDEV, $\sigma = 1.08 \mu\text{m}/\text{min}$) and for C14 was $4.2 \pm 0.30 \mu\text{m}/\text{min}$ (STDEV, $\sigma = 0.95 \mu\text{m}/\text{min}$). The critical value of *F* at 95% probability level was much

TABLE 2
COMPARISON OF THE GROWTH RATES OF THE PARENTAL CELL LINE (MB35) AND THE RECOMBINANT CELL LINES USING STUDENT'S *t*-TEST ON (*N* - 1) DEGREES OF FREEDOM

Compared Cell Lines	Mean Slope	SE of the Slopes	Student's <i>t</i> Test Values	<i>p</i> -Values (<i>N</i> = 3)
MB35 (parent) and C4	452733.01 81351.38	6083.71 2419.98	56.72	0.000159
MB35 (parent) and C7	452733.01 48573.78	6083.71 6291.02	46.18	0.000001
MB35 (parent) and C14	452733.01 41106.16	6083.71 2229.24	62.94	0.000126

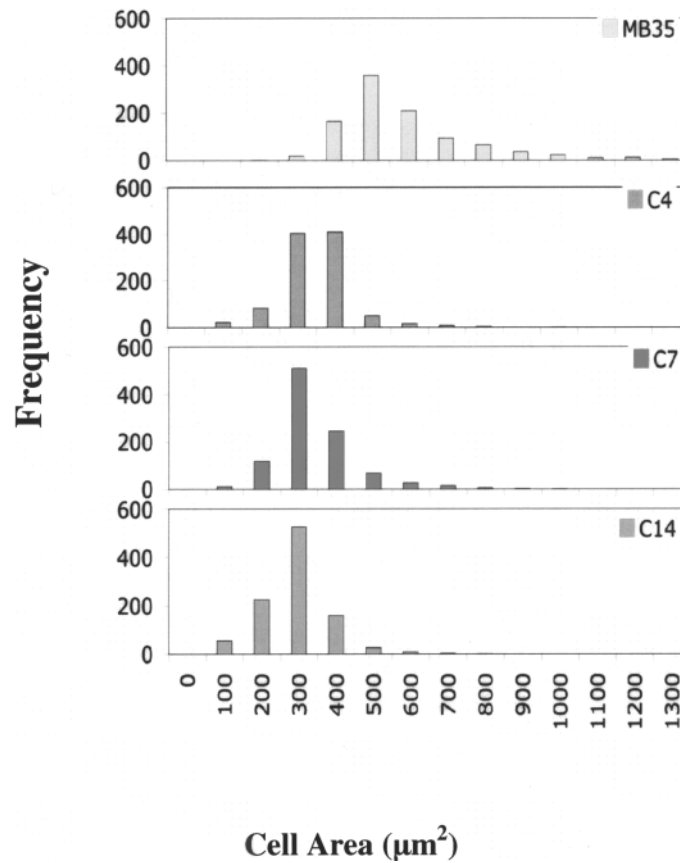


Figure 4. Cell size of the cell lines compared with MB35 cell line. The area of majority of the parental cells was within the range of 400–600 μm^2 while most of the cells of C4 cell line were within the range of 200–400 μm^2 . Likewise, the majority of the cells of cell lines C7 and C14 were within the range of 200–300 μm^2 .

higher (F -crit = 2.866) than the observed value of F (F -observed = 0.567).

The average cell speed at 6.5 h of starvation for MB35 of 6.59 ± 0.70 $\mu\text{m}/\text{min}$ (STDEV, $\sigma = 2.23$ $\mu\text{m}/\text{min}$), C4 of 6.23 ± 0.66 $\mu\text{m}/\text{min}$ (STDEV, $\sigma = 2.11$ $\mu\text{m}/\text{min}$), C7 of 4.45 ± 0.36 $\mu\text{m}/\text{min}$ (STDEV, $\sigma = 1.16$ $\mu\text{m}/\text{min}$), and C14 of 4.39 ± 0.32 $\mu\text{m}/\text{min}$ (STDEV, $\sigma = 1.02$ $\mu\text{m}/\text{min}$) was noted. The difference in cell speed at this time point was subtle but significant ($n = 10$, $p = 0.0087$) as the critical value of F at 95% probability level was much lower (2.866) than the observed value of F (F -observed = 4.51).

Development Assay

Starvation induces *Dictyostelium* amoebae to undergo a developmental cycle whereby approximately 10^5 amoebae aggregate and then differentiate to form a multicellular fruiting body. The entire developmental cycle was completed (aggregation of amoebae to fruiting body formation) in 24 h following starvation and was marked by distinct phenotypic stages at different time points (Fig. 8). The recombinant cell

lines and the parental cells were compared at two different stages of development: loose aggregate stage (10 h) and fruiting body stage (24 h). At 10 h of starvation the amoebae formed a loose aggregate and get arranged in concentric circles and at 24 h following starvation, a fruiting body with a stalk and a spore was formed.

After 10 h of starvation, MB35 cells got arranged in a concentric pattern (Fig. 8) but the recombinant cell lines (C4, C7, and C14) were poorly aggregated as irregular masses of cells. At 24 h of starvation, a mature fruiting body was formed by the starving MB35 cells, but recombinant cells were at the tight aggregation stage that in normal starving cells occurs at 12–14 h of starvation. At 48 h of starvation, the recombinant cells formed a finger-like structure called migrating slug stage, which normally occurs at 16–18 h of starvation. The development of recombinant cell lines was followed beyond 48 h and it was found that the fruiting bodies were formed after 58 h of starvation (data not shown), but they were very small compared to the fruiting bodies of the parental cells. Thus, a significant delay in the development

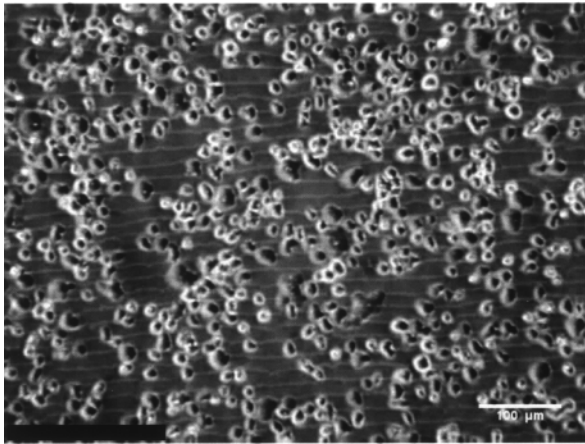


Figure 5 a: MB35 parental cell

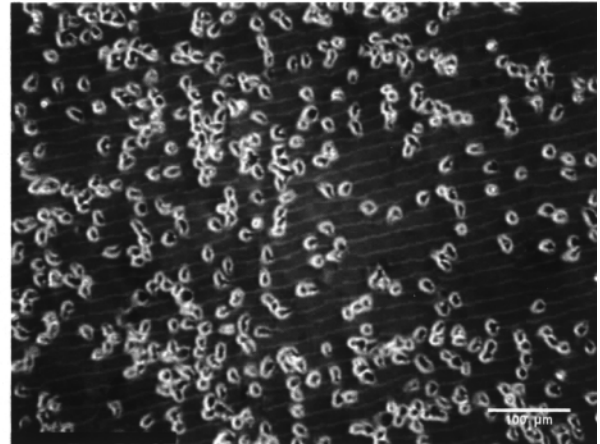


Figure 5b: C4 cell line

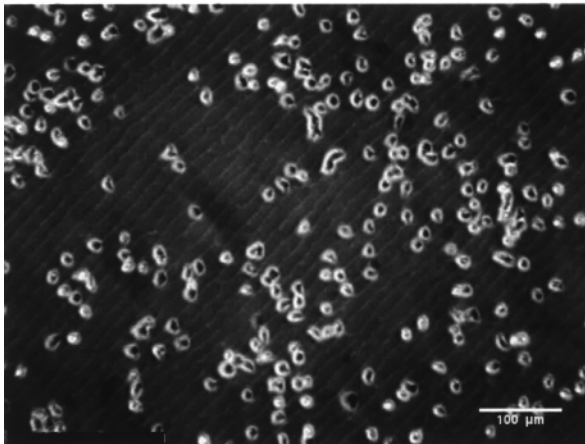


Figure 5c: C7 cell line

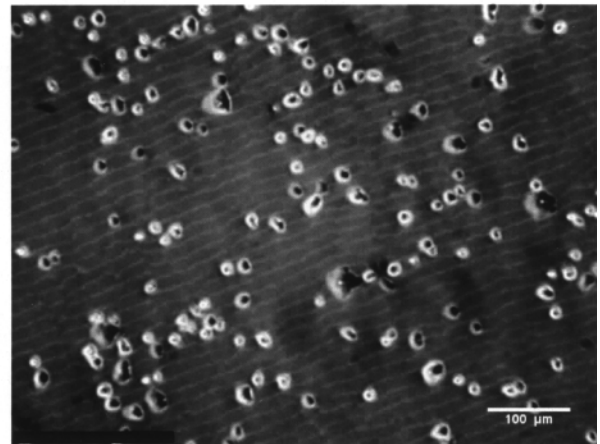


Figure 5d: C14 cell line

Figure 5. Cell size comparison. A representative image for each cell line used for cell size analysis. MB35 (a), C4 (b), C7 (c), and C14 (d). Scale bars: 100 μm .

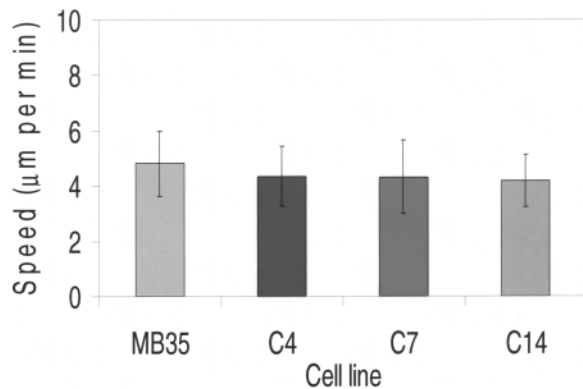


Figure 6. Average cell speed of MB35 (parental cells) and the *Dd-grp94* RNAi recombinant cell lines at 5.5 h of starvation ($n = 10$, $p = 0.640$). SD: MB35 = ± 1.067 , C4 = ± 1.08 , C7 = ± 1.33 , C14 = ± 0.95 . ($F\text{-crit} = 2.866 > F\text{-observed} = 0.567$).

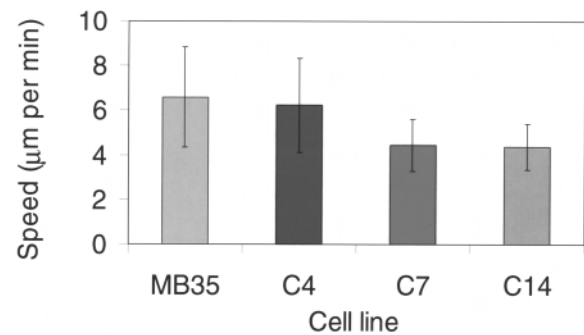


Figure 7. Average cell speed of MB35 (parental cells) and the *Dd-grp94* RNAi recombinant cell lines at 6.5 h of starvation ($n = 10$, $p = 0.0087$). SD: MB35 = ± 2.23 , C4 = ± 2.11 , C7 = ± 1.16 , C14 = ± 1.02 ($F\text{-crit} = 2.86 < F\text{-observed} = 4.515$).

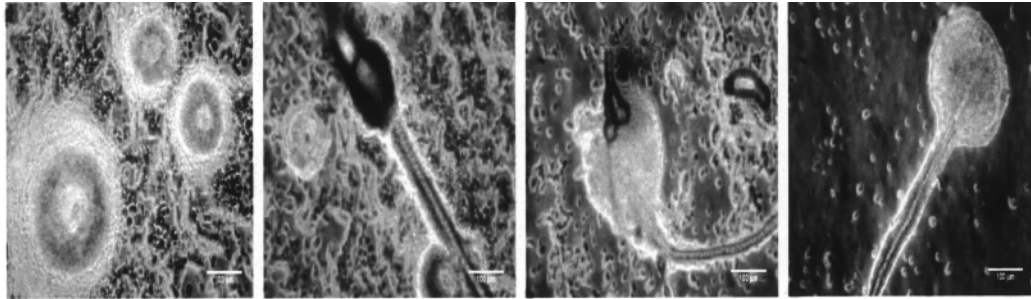
MB35 (Parental cells)

10 Hours

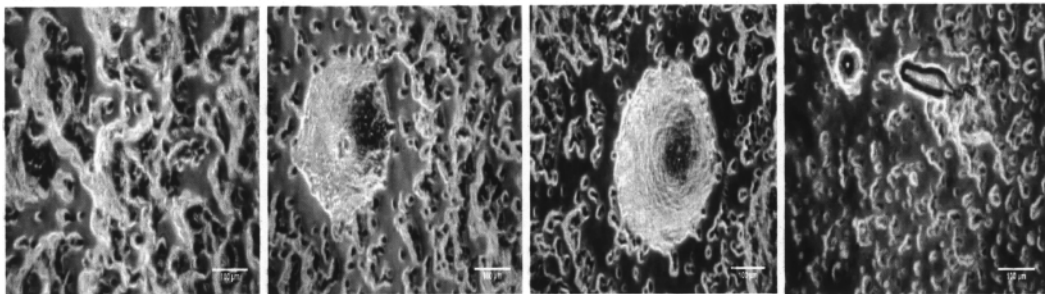
24 Hours

36 Hours

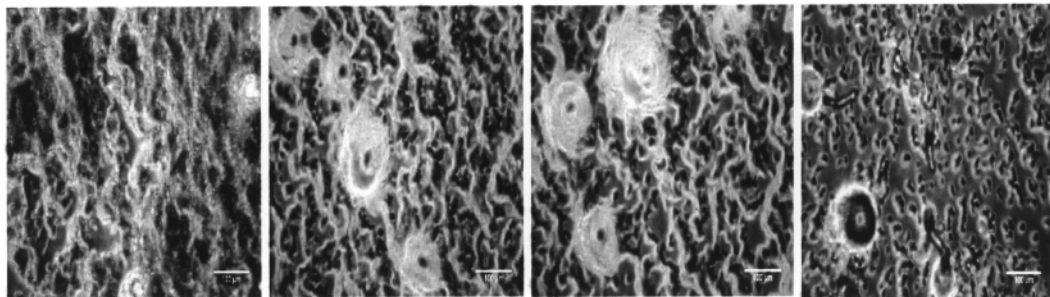
48Hours



C4



C7



C14

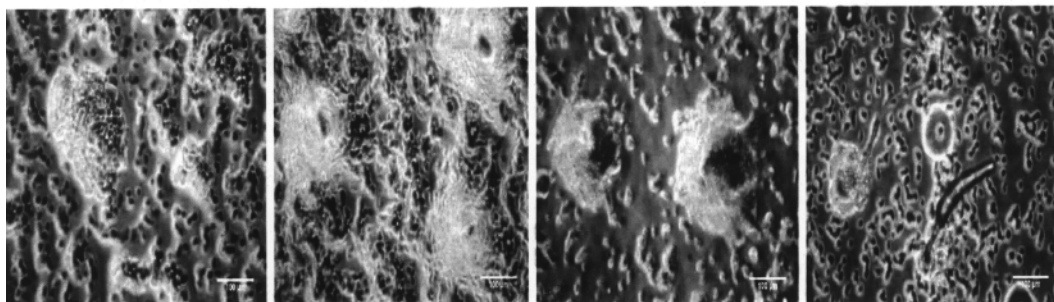


Figure 8. Development of the *Dd-grp94* RNAi recombinants and MB35 (parental cell line) at different time points. Scale bars: 100 µm.

(approximately 20 h) and the reduction in the size of the fruiting bodies was observed when development of the parental and recombinant cell lines were compared.

DISCUSSION

We report here reduction in cell size and proliferation rate as well as delay in development as consequences of *Dd-Grp94* downregulation.

Cell Proliferation and Cell Size

The cytoskeleton is made up of three types of filament proteins: microfilaments, microtubules, and intermediate fibers. The actin microfilaments (F-actin) are formed by reversible polymerization of monomeric actin molecules called G-actin (11). The actin proteins constitute about 8% of total cellular proteins in *Dictyostelium* and in resting *Dictyostelium* cell G-actin (monomer) and F-actin (polymer) molecules occur in equal ratio as certain cellular factors maintain a balance between actin monomers and polymers (30). The actin filaments are cross-linked by a variety of proteins known as filament cross-linkers or F-actin binding proteins. These cytosolic proteins, which are large and elongated, are regulated by calcium, phospholipids, phosphorylated proteins, pH (11,13), and other changes in extracellular and intracellular environment of the cell. The proteins make the cytoplasm very dynamic by controlling polymerization of G-actin monomers into filaments within seconds of receiving a signal (24) and by binding to the actin filaments with different affinities. The dynamic nature of the cytoskeleton helps the cell maintain its size and perform different processes such as cell division, migration, and differentiation. The F-actin cross-linking proteins in *Dictyostelium*, which are regulated by calcium, belong to the α -actinin/spectrin superfamily of proteins (13). These proteins are α -actinin, filamin/ABP240, fodrin/ABP220, the gelation factor/ABP120, cortaxillin I and II, fimbrin, and interaptin. Most of these proteins have been characterized and their mutants show defect either in cytokinesis or in development (7,36,48).

Two cytoskeletal proteins, namely α -actinin and the gelation factor, are relevant to the current study as the knock-out mutants of these proteins show reduced growth rate and cell size similar to the *Dd-grp94* RNAi recombinants (7). Rivero et al. (36) indicated that reduced growth rate and cell size in mutants could be due to inability of the cytoskeleton (due to reduced strength) to resist internal forces during growth, which ultimately results in smaller cell size. Because knock-out mutants of α -actinin and the gelation factor and *Dd-grp94* RNAi recombinants exhibit

similar phenotypes, we propose that *Dd-Grp94*, α -actinin, and the gelation factor belong to the same signaling pathway that regulates growth rate in *Dictyostelium*.

Cell Speed

Chemotaxis and cell motility are important processes of vegetative and developmental phases of *D. discoideum* life cycle (18,39). Chemotaxis is orientation of cells in relation to chemoattractants like folic acid and cAMP. During the vegetative phase, *D. discoideum* cells migrate towards bacteria (food) in response to folic acid secreted by bacteria (50). Upon starvation, the amoebae secrete cAMP and signal the neighboring cells to aggregate and form fruiting body (9,43). Both the chemoattractants are responsible for directed migration and bind to the cell surface receptors, which lead to several biochemical changes inside the cell such as increased level of cGMP and calcium, which then leads to dramatic reorganization of actin cytoskeleton, resulting in the extension of pseudopodia in new direction and consequently change in the direction of migration (39). Besides cAMP, various other factors such as cell density, temperature, light, and moisture affect movement and aggregation of *Dictyostelium* amoebae (18).

For measuring the cell speed, starving amoebae (approximately 1×10^6) were evenly spread on a 100-mm petri dish and the movement of cells was video recorded for 30 min but the direction of the cell movement was not controlled in this measurement. The incremental distance traveled by a cell between frames was measured instead of measuring the total distance covered by the cell over the entire 30-min interval. The average cell speed was calculated as a mean of the distances traveled by a cell from one frame to the next (for 40 frames) divided by the single frame time interval (45 s).

No significant difference was observed between the cell speeds of recombinants and the parental cells. Cell speeds were also found to vary greatly within the individual cell lines. While a small downward trend in cell speed (34% reduction in mean speed of recombinants compared to the control at 6.5 h of starvation) was seen, the inherent variability of the measurement makes any conclusion regarding the effect of downregulation of *Dd-Grp94* on cell speeds of recombinants problematic. This is partly because critical variables affecting cell movement such as cell density and cAMP concentration were not controlled during the measurement, and the measurements were only done with 10 cells per cell line.

Considering the above limitations of measurement, it was expected that the cell speeds of the *Dd-grp94* downregulated recombinants (C4, C7, and C14)

would have to be less than half that of the control cell line to be statistically significant. However, this is merely an artifact of the measurement accuracy, because any reduction in motility could in fact be biologically “significant.”

The fact that the development of recombinants was affected at the aggregation stage and beyond suggests that cell motility of the recombinants might have been affected. The *Dd-grp94* RNAi recombinants exhibited significant delay in the development (approximately 20 h) and small fruiting bodies. Even a moderate reduction in cell speed can significantly delay the development because every stage of the development involves large scale movement of the cells. For example, control cells which move at a normal speed (10 $\mu\text{m}/\text{min}$) would aggregate and attain all the stages of development in a timely manner but recombinant cells with a moderately reduced speed (e.g., 7 $\mu\text{m}/\text{min}$) would show progressive delay at every stage of the development and hence complete the developmental cycle very late or fail to complete the cycle at all. In other words, the rate of movement could reflect a biological threshold of which we are ignorant.

Development

Morita et al. (27) studied the expression level of *Dd-grp94* in wild-type *D. discoideum* (AX2 strain) cells and found that the level of *Dd-Grp94* protein varies at different time points during the development. They noted that during the first hour of starvation, *Dd-Grp94* level decreases rapidly and remain low until 4 h of starvation but increases rapidly (2–3 times more than its level at the vegetative phase) between 8 and 10 h of starvation, which coincides with the loose aggregate stage of the development. At 12–14 h of starvation, *Dd-Grp94* level is hardly detectable. This means that at loose aggregate stage, *Dd-Grp94* plays important role.

When the development of *Dd-grp94* RNAi recombinants was examined at the loose aggregate stage (10 h of starvation), the recombinant cells had formed irregular masses and not the concentric pattern that is typical of the same stage in wild-type cells. It appeared that the recombinant cells may have formed irregular masses due to cell–cell adhesion rather than aggregation following chemotaxis to cAMP. It is possible that cAMP synthesis and its amplification relay among neighbors is affected due to downregulation of *Dd-Grp94*.

The *car1* gene expresses a cell-surface receptor protein called cAMP receptor protein1 in response to cAMP (22,37). If *car1* expression were depressed following downregulation of *Dd-Grp94* then cell aggregation might logically be delayed. Further investigation is required to determine if the *Dd-grp94* and *car1* genes belong to the same signaling pathway or regulatory complex. This would contribute towards understanding the complex regulatory network in which *Dd-Grp94* protein functions.

ACKNOWLEDGMENTS

We would like to thank Dr. Curt Anderson, Department of Biological Sciences, Idaho State University, for providing his expertise in image analysis and for making the facilities available of his lab. We acknowledge Dicty Stock Center, Northwestern University, Chicago, for providing *Dictyostelium* MB35 cells (strain ID: DBS0236537) and pMB38 extrachromosomal response plasmid (strain ID: 45). We also acknowledge Molecular Research Core Facility (MRCF) and Graduate Student Research and Scholarship Committee (Grant No. S05-102), Idaho State University, for providing the funding and the facilities to complete the project.

REFERENCES

1. Alastair, E. C.; Peyrou, M.; Shamugum, M. The endoplasmic reticulum in xenobiotic toxicity. *Drug Metab. Rev.* 37:405–442; 2005.
2. Argon, Y.; Simen, B. GRP94, an ER chaperone with protein and peptide binding properties. *Cell Dev. Biol.* 10:495–505; 1999.
3. Bando, Y.; Katayama, T.; Kasai, K.; Taniguchi, M.; Tamatani, M.; Tohyama, M. GRP94 (94 kDa glucose-regulated protein) suppresses ischemic neuronal cell death against ischemia/reperfusion injury. *Eur. J. Neurosci.* 18:829–840; 2003.
4. Biswas, C.; Ostrovsky, O.; Makarewich, C.; Wanderling, S.; Gidalewitz, T.; Argon, Y. The peptide-binding activity of GRP94 is regulated by calcium. *Biochem. J.* 405:233–241; 2007.
5. Boeckeler, K.; Tischendorf, G.; Mutzel, R.; Weissenmayer, B. Aberrant stalk development and breakdown of tip dominance in *Dictyostelium* cell lines with RNAi-silenced expression of calcineurin B. *BMC Dev. Biol.* 6:12; 2006.
6. Bretschneider, T.; Jonkman, J.; Köhler, J.; Medalia, O.; Barisic, K.; Weber, I.; Stelzer, E. H.; Baumeister, W.; Gerisch, G. Dynamic organization of the actin system in the motile cells of *Dictyostelium*. *J. Muscle Res. Cell Motil.* 23:639–649; 2002.
7. Brink, M.; Gerisch, G.; Isenberg, G.; Noegel, A. A.; Segall, J. E.; Wallraff, E.; Schleicher, M. A. *Dictyostelium* mutant lacking an F-actin cross-linking protein, the 120kD gelation factor. *J. Cell Biol.* 111:1477–1489; 1990.
8. Chida, J.; Amagai, A.; Tanaka, M.; Maeda, Y. Establishment of a new method for precisely determining

- the functions of individual mitochondrial genes, using *Dictyostelium* cells. *BMC Genet.* 9:25; 2008.
9. Deveotes, P. N.; Zigmond, S. H. Chemotaxis in eukaryotic cells: A focus on leukocytes and *Dictyostelium*. *Annu. Rev. Cell Biol.* 4:649–686; 1988.
 10. Dollins, D. E.; Warren, J. J.; Immormino, R. M.; Gewirth, D. T. Structures of GRP94-nucleotide complexes reveal mechanistic differences between the hsp90 chaperones. *Mol. Cell* 28:41–56; 2007.
 11. Eichinger, L.; Lee, S.; Schleicher, M. *Dictyostelium* as model system for studies of the actin cytoskeleton by molecular genetics. *Microsc. Res. Techn.* 47:124–134; 1999.
 12. Eichinger, L.; Pachebat, J. A.; Glockner, G.; Rajandream, M. A.; Sugang, R.; Berriman, M.; Song, J.; Olsen, R.; Szafranski, K.; Xu, Q., et al. The genome of the social amoeba *Dictyostelium discoideum*. *Nature* 435:43–57; 2005.
 13. Furukawa, R.; Maselli, A.; Thomson, S. A. M.; Lim, R. W. L.; Stokes, J. V.; Fechtmeier, M. Calcium regulation of actin crosslinking is important for function of the actin cytoskeleton in *Dictyostelium*. *J. Cell Sci.* 116:187–196; 2003.
 14. Ishiguro, S.; Watanabe, Y.; Ito, N.; Nonaka, H.; Takeda, N.; Sakai, T.; Kanaya, H.; Okada, K. SHEPHERD is the Arabidopsis GRP94 responsible for the formation of functional CLAVATA proteins. *EMBO J.* 21:898–908; 2002.
 15. Kang, H.; Welch, W. Characterization and purification of the 94-kDa glucose-regulated protein. *J. Biol. Chem.* 266:5643–5649; 1991.
 16. Kaufman, R. J. Molecular chaperones and heat shock response. *Biochem. Biophys. Acta* 1423:R13–R27; 1999.
 17. Kessin, R.; VanLookeren Campagne, M. The development of a social amoeba. *Am. Sci.* 80; 1992.
 18. Kessin, R. H. *Dictyostelium*: Evolution, cell biology, and the development of multicellularity. New York: Cambridge University Press; 2001.
 19. Kitanishi-Yumura, T.; Fukui, Y. Actomyosin organization during cytokinesis: Reversible translocation and differential redistribution in *Dictyostelium*. *Cell Motil. Cytoskel.* 12:78–89; 1989.
 20. Lee, A. S. The glucose regulated proteins: Stress induction and clinical applications. *Trends Biochem. Sci.* 26:504–510; 2001.
 21. Loomis, W. F.; Kuspa, A. *Dictyostelium* genomics. Horizon Bioscience; August 2005.
 22. Mann, S. K.; Pinko, C.; Firtel, R. A. Control of early gene expression in *Dictyostelium*. *Dev. Genet.* 9:337–350; 1989.
 23. Martens, H.; Novotny, J.; Oberstrass, J.; Steck, T. L.; Postlethwait, P.; Nellen, W. RNAi in *Dictyostelium*: The role of RNA-directed RNA polymerases and double-stranded RNase. *Mol. Biol. Cell* 13:445–453; 2002.
 24. McRobbie, S. J.; Newell, P. C. Effects of cytochalasin B on cell movements and chemoattractant-elicited actin changes of *Dictyostelium*. *Exp. Cell Res.* 160:275–286; 1985.
 25. Melnick, J.; Dul, J.; Argon, Y. Sequential interaction of the chaperones BiP and GRP94 with immunoglobulin chains in the endoplasmic reticulum. *Nature* 370:373–375; 1994.
 26. Moniakis, J.; Coukell, M. B.; Janice, A. Involvement of the Ca²⁺-ATPase PAT1 and the contractile vacuole in calcium regulation in *Dictyostelium discoideum*. *J. Cell Sci.* 112:405–414; 1999.
 27. Morita, T.; Saitoh, K.; Takagi, T.; Maeda, Y. Involvement of the glucose-regulated protein 94 (DdGRP94) in starvation response of *Dictyostelium discoideum* cells. *Biochem. Biophys. Res. Commun.* 274:323–331; 2000.
 28. Muresan, Z.; Arvan, P. Thyroglobulin transport along the secretory pathway—investigation of the role of molecular chaperone, GRP94, in protein export from the endoplasmic reticulum. *J. Biol. Chem.* 272:26095–26102; 1997.
 29. Newell, P. C.; Malchow, D.; Gross, J. D. The role of calcium in aggregation and development of *Dictyostelium*. *Experientia* 51:1155–1165; 1995.
 30. Podolski, J. L.; Steck, T. L. Length distribution of F-actin in *Dictyostelium discoideum*. *J. Biol. Chem.* 265:1312–1318; 1990.
 31. Randow, F.; Seed, B. Endoplasmic reticulum chaperone gp96 is required for innate immunity but not cell viability. *Nat. Cell Biol.* 3:891–896; 2001.
 32. Rasband, W. S. ImageJ. Bethesda, MD: U.S. National Institutes of Health; 2008.
 33. Rathi, A.; Kayman, S. C.; Clarke, M. Induction of gene expression in *Dictyostelium* by prestarvation factor, a factor secreted by growing cells. *Dev. Genet.* 12:82–87; 1991.
 34. Reddy, R.; Dubeau, L.; Kliener, H.; Parr, T.; Nichols, P.; Ko, B.; Dong, D.; Ko, H.; Mao, C.; DiGiovanni, J., et al. Cancer-inducible transgene expression by the Grp94 promoter: Spontaneous activation in tumors of various origins and cancer-associated macrophages. *Cancer Res.* 62:7207–7212; 2002.
 35. Reed, R.; Zheng, T.; Nicchitta, C. GRP94-associated enzymatic activities. *J. Biol. Chem.* 277:25082–25089; 2002.
 36. Rivero, F.; Köppel, B.; Peracino, B.; Bozzaro, S.; Siegert, F.; Weijer, C. J.; Schleicher, M.; Albrecht, R.; Noegel, A. A. The role of the cortical cytoskeleton: F-actin crosslinking proteins protect against osmotic stress, ensure cell size, cell shape and motility, and contribute to phagocytosis and development. *J. Cell Sci.* 109:2679–2691; 1996.
 37. Saxe, 3rd, C. L.; Johnson, R. L.; Devreotes, P. N.; Kimmel, A. R. Expression of a cAMP receptor gene of *Dictyostelium* and evidence for a multigene family. *Genes Dev.* 5:1–8; 1991.
 38. Schlatterer, C.; Knoll, G.; Malchow, D. Intracellular calcium during chemotaxis of *Dictyostelium discoideum*: A new fura-2 derivative avoids sequestration of the indicator and allows long-term calcium measurements. *Eur. J. Cell Biol.* 58:172–181; 1992.
 39. Segall, J. E.; Fisher, P. R.; Gerisch, G. Selection of chemotaxis mutants of *Dictyostelium discoideum*. *J. Cell Biol.* 104:151–161; 1987.

40. Soldano, K. L.; Jivan, A.; Nicchitta, C. V.; Gewirth, D. T. Structure of the N-terminal domain of GRP94: Basis for ligand specificity and regulation. *J. Biol. Chem.* 278:48330–48338; 2003.
41. Stoilova, D.; Dai, J.; de Crom, R.; van Haperen, R.; Li, Z. Haplosufficiency or functional redundancy of a heat shock protein gp96 gene in the adaptive immune response. *Cell Stress Chaperones* 5:395; 2000.
42. Stossel, T. P. On the crawling of animal cells. *Science* 260:1086–1094; 1993.
43. Varnum, B.; Soll, D. R. Effects of cAMP in *Dictyostelium* on single cell motility. *J. Cell Biol.* 99:1151–1155; 1984.
44. Verkhatsky, A.; Toescu, E. Endoplasmic reticulum calcium homeostasis and neuronal death. *J. Cell. Mol. Med.* 7:351–361; 2003.
45. Vitadello, M.; Penzo, D.; Petronilli, V.; Michieli, G.; Gomirato, S.; Menabo, R.; Di Lisa, F.; Gorza, L. Overexpression of the stress protein Grp94 reduces cardiomyocytes necrosis due to calcium overload and simulated ischemia. *FASEB J.* 17:923–925; 2003.
46. Wanderling, S.; Simen, B. B.; Ostrovsky, O.; Ahmed, N. T.; Vogen, S. M.; Gidalevitz, T.; Argon, Y. GRP94 is essential for mesoderm induction and muscle development because it regulates insulin-like growth factor secretion. *Mol. Biol. Cell* 18:3764–3775; 2007.
47. Wang, Q.; Lija, A.; Chen, Y.; Yue, S. Expression of endoplasmic reticulum molecular chaperon GRP94 in human lung cancer tissues and its clinical significance. *Chin. Med. J.* 115:1615–1619; 2002.
48. Witke, W.; Schleicher, M.; Noegel, A. A. Redundancy in the microfilament system: Abnormal development of *Dictyostelium* cells lacking two F-actin cross-linking proteins. *Cell* 68:53–62; 1992.
49. Yang, Y.; Li, B.; Dai, J.; Srivastava, P. K.; David, J.; Zammit, D. J.; Lefrançois, L.; Li, Z. Heat shock protein gp96 is a master chaperone for toll-like receptors and is important in the innate function of macrophages. *Immunity* 26:215–226; 2007.
50. Yumura, S.; Furuya, K.; Takeuchi, I. Intracellular free calcium responses during chemotaxis of *Dictyostelium* cells. *J. Cell Sci.* 109:2673–2678; 1996.
51. Zofia, W.; Happle, K.; Muller-Taubenberger, A.; Schlatter, C.; Malchow, D.; Fisher, P. Release of Ca²⁺ from endoplasmic reticulum contributes to Ca²⁺ signaling in *Dictyostelium discoideum*. *Eukaryotic Cell* 4:1513–1525; 2005.

